31st Annual International Conference of the IEEE EMBS
Minneapolis, Minnesota, USA, September 2-6, 2009

Modeling Bimodal Vessel Effects on Radio and Microwave Frequency Ablation Zones

Joseph D. Brannan, *Member, IEEE,* Casey M. Ladtkow

***Abstract*—A bench liver model is presented that separates the thermal and electrical effects of large blood vessels within radio and microwave frequency ablation boundaries. The model includes a cylindrical tissue environment with a 5 mm vessel placed parallel to and 15 mm way from either a Covidien Energy-based Devices Evident™ MW Ablation Percutaneous Antenna or a CoolTip™ RF Ablation Single Electrode Kit. An array of fiber optic thermal probes is used to monitor radial temperature profile on the vessel and non-vessel sides of the ablation zone. Circulating blood exhibits higher electrical conductivity than surrounding liver tissue and provides a significant means for transport of thermal energy. Data from the thermal probes indicate key performance differentiators between MW and RF ablation modalities when they are used next to large blood vessels clarifying the difference between thermal and electrical energy sink. The results suggest RFA is susceptible to both the thermal and electrical energy sink effects of large vasculature while MWA is only susceptible to thermal sink. Ablation zone boundaries were distorted on both the vessel and non-vessel sides with RFA whereas with MWA only the vessel side is affected.**

I. Introduction

HIGH temperature thermal ablation of primary and metastatic liver tumors is a common therapy for patients who are not good candidates for surgical resection. Several energy modalities are available for thermal ablation including radiofrequency ablation (RFA) and microwave ablation (MWA). The frequency of operation differs by at least one order of magnitude between these two options, which results in differentiating factors with respect to device tissue effect. MWA offers key advantages over RFA including higher treatment temperatures, larger active heating zone and reduced susceptibility to ablation zone distortion when used near large vasculature [1]. Vessels with active blood circulation are large thermal sinks and display higher electrical conductivity than surrounding tissue. The vessel model in this study exaggerates actual physiological conditions. This study examines individually thermal effects and electrical effects of large vasculature on ablation performance in both RFA and MWA. It should not be used to compare RFA and MWA ablation size.

Manuscript received April 7, 2009. This work was supported by Covidien Energy-based Devices, Boulder Colo. USA. J.D. Brannan and C.M. Ladtkow are with Covidien Energy-based Devices Boulder, CO 80301 USA (email: joseph.brannan @ covidien.com).

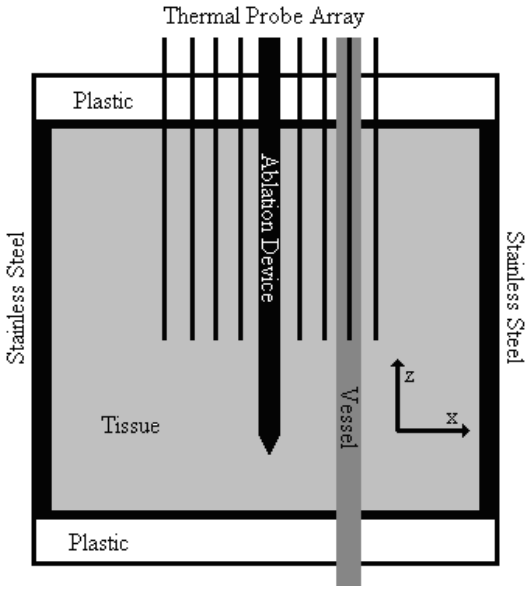

Fig. 1: Cross section of bench model.

II. Methods

The bench model for this study utilized coarsely ground fresh ex-vivo bovine liver tissue. After grinding, tissue was immediately placed on ice for transport and then stored at a temperature between 15-17°C up to the time of use, which was within 24 hours of excision.

The schematic representation of the fixture used for the bench liver model in this study is shown in Fig. 1. The fixture is cylindrical in the z direction. The ablation device is inserted into the fixture such that the largest width in the x-y plane of the resulting ablation resides in the center of the tissue volume. A fiber-optic thermal probe array with non-conductive cannulas is situated to acquire temperature data in the x-y plane corresponding to maximum ablation zone diameter. Thermal probe spacing is every 5 mm out to a 20 mm radius from the fixture center on either side of the ablation probe.

Four separate configurations of the fixture provide control, thermal, conductive and combined measurement cases for vessel effect modeling. The control case does not contain a vessel structure. The thermal case uses a 5 mm diameter 1 mm wall thickness glass tube with circulating water for the vessel structure. The conductive case uses a 5 mm diameter 1 mm wall thickness stainless steel tube with stagnant water for the vessel structure. The combined case uses the stainless steel tube with circulated water. The

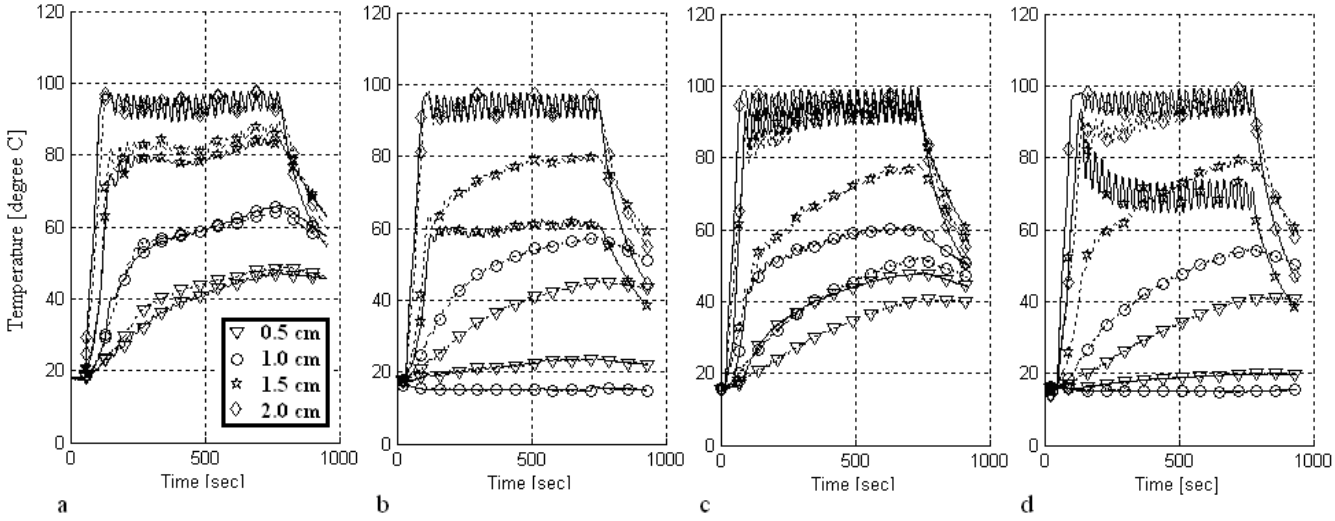

Fig. 2: RFA thermal array data. Dashed line indicates opposite side of vessel, solid line indicates same side as vessel. (a) control (b) thermal (c) conductive (d) combined

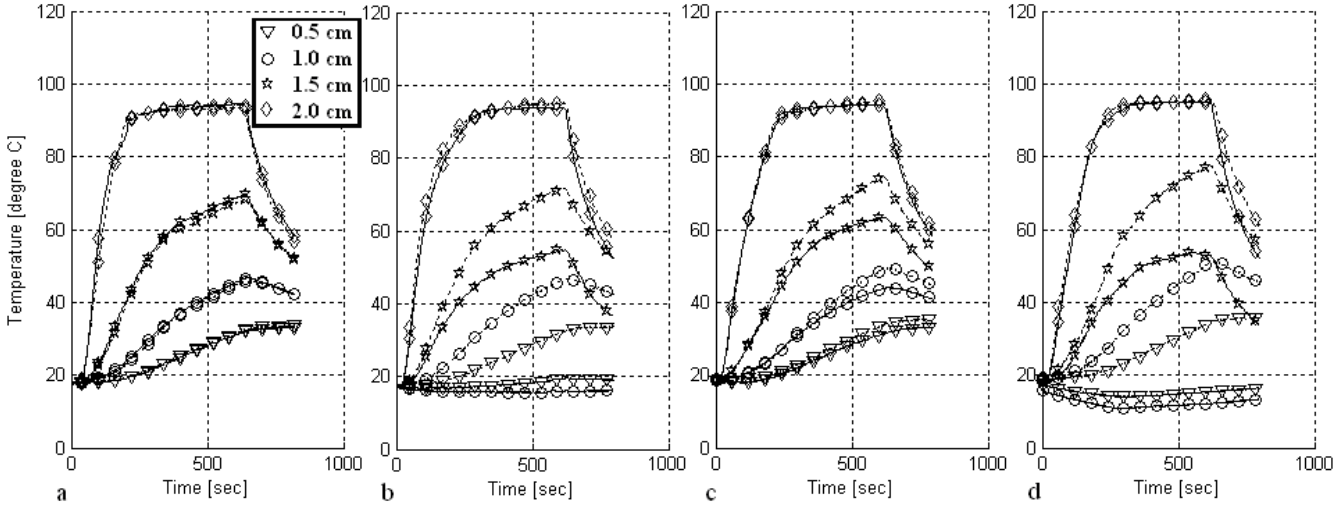

Fig. 3: MWA thermal array data. Dashed line indicates opposite side of vessel, solid line indicates same side as vessel. (a) control (b) thermal (c) conductive (d) combined

thermal probe associated with the vessel position was inserted into the vessel tube to a position consistent with the array. A pump maintained 1 L per minute flow rate of 15-18°C tap water through the tubes for the thermal and combined cases. For conductive and combined cases, the stainless steel tube and stainless steel cylinder are electrically connected with an electrical wire. During RFA ablation, the return electrode was the combination of the stainless steel tube and cylinder.

Ablations were performed using the Evident™ MW Ablation Percutaneous Antenna or a CoolTip™ RF Ablation Single Electrode Kit (both Covidien, Boulder Colo). Generator settings were consistent with instructions for use (IFU) parameters. For MWA, 45 watts of 915 MHz forward power were delivered to the device for 10 minutes. For RFA, the CoolTip™ RF ablation system algorithm (Covidien, Boulder Colo.) delivered 470 kHz energy to the device for 12 minutes. Measurement trials were randomized within the RFA and MWA groups. Three ablations were

TABLE I
TRENDS IN ABLATION ZONE RADIUS WITH RESPECT TO CONTROL: NON VESSEL SIDE / VESSEL SIDE

	Thermal	Electrical	Combined
RFA	None/Smaller	Smaller/None	Smaller/Smaller
MWA	None/Smaller	None/None	None/Smaller

TABLE II
STATISTICAL SHIFT IN ABLATION ZONE RADIUS FROM CONTROL: NON VESSEL SIDE / VESSEL SIDE

	Thermal	Electrical	Combined
RFA	None/Smaller	Smaller/None	None/Smaller
MWA	None/Smaller	None/None	None/Smaller

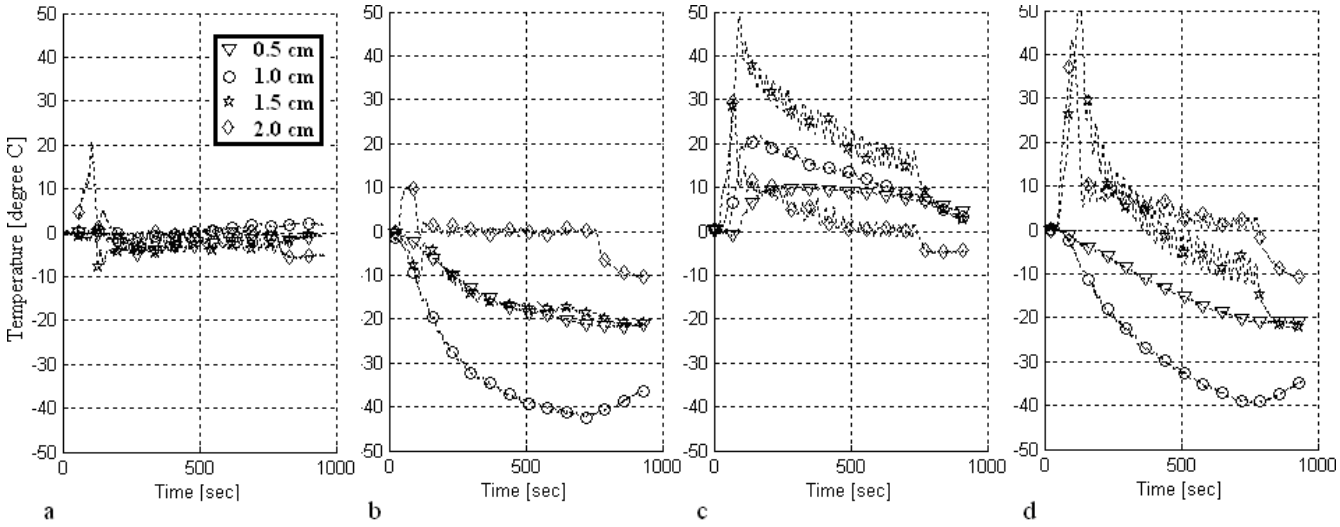

Fig. 4: RFA thermal array data. Temperature toward vessel minus away from vessel. (a) control (b) thermal (c) conductive (d) combined

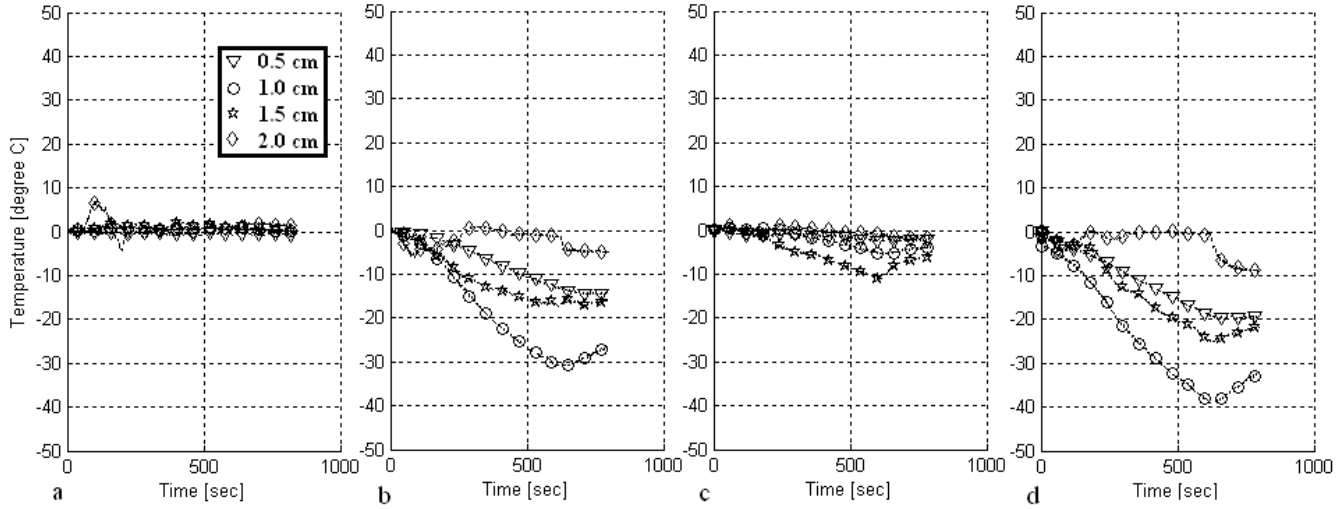

Fig. 5: MWA thermal array data. Temperature toward vessel minus away from vessel. (a) control (b) thermal (c) conductive (d) combined

performed for each energy type and model combination. Fresh tissue replaced used tissue after each trial. Thermal array data was used to calculate ablation boundaries using the Arrhenius method [2-4].

III. Results

Data acquired from the thermal array during select MWA measurement trials is displayed in Fig. 2 and select RFA results are displayed in Fig. 3. Select ablation results are displayed as examples for each model case (control, thermal, conductive, combined) and energy type (RFA, MWA). Trends observed in thermal behavior were consistent for each energy type/model case combination, as shown in Table 1. Fig. 4 and Fig. 5 display the difference in measured temperature across symmetric pairs of thermal probes in the array for the data shown in Figs. 2 and 3. Fig. 6 is a bar chart with 95% confidence interval on the mean for ablation boundary radius to either side of the probe along the thermal array for all data.

IV. Discussion

Vasculature within bench liver models often causes non-symmetric ablation zones. Using ground tissue for the model in this study enabled observation of spatially symmetric x-y plane thermal ablation behavior in the control case for both RFA and MWA by eliminating the presence of intact vasculature. The non-symmetric heating pattern in the three vessel model cases is therefore due to the prescribed vessel effect, not inhomogeneous tissue.

During ablations performed in the thermal case for both RFA and MWA, tissue temperature at radii of 10 mm, 15mm and 20 mm on the vessel side of the ablation was lower than the corresponding non-vessel side. Tissue temperature at the 5 mm radius was symmetrical. The tissue temperature to the vessel side of the ablation is lower due transport of thermal energy away from the ablation site by the flowing 15-17°C water within the vessel. Tissue

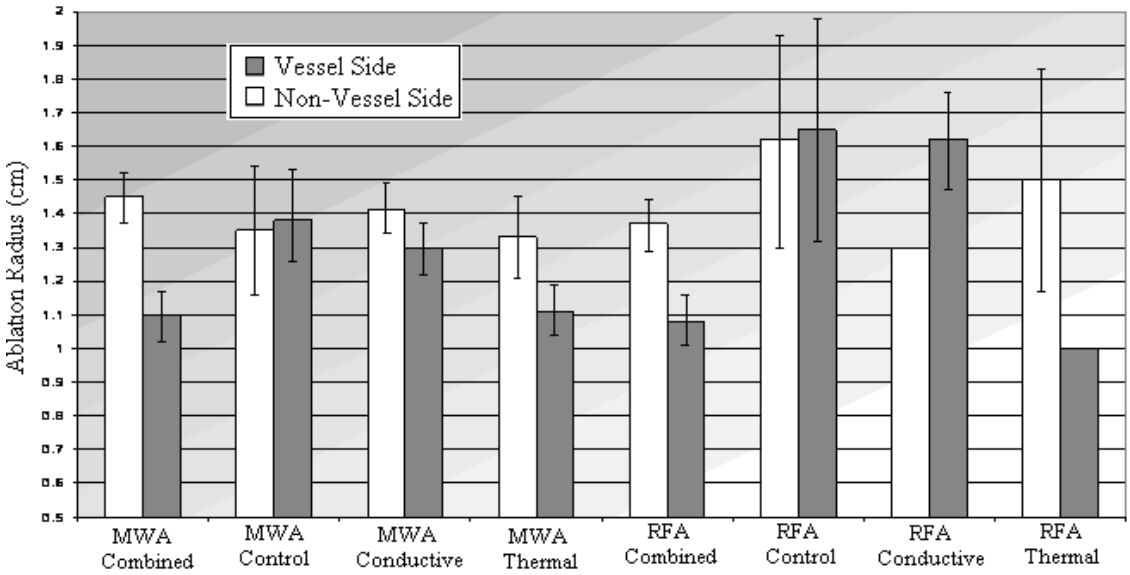

Fig. 6: Mean of ablation radius along thermal array, 95% confidence interval included.

temperature within 5 mm of the ablation devices was not close enough to the vessel to be affected by the thermal sink.

Ablations performed in the conductive case are perhaps the most interesting results of this study. In the RFA ablations, tissue temperatures at all probe positions on the vessel side of the thermal array were elevated with respect to the non-vessel side due to comparatively higher current densities. The conductive 'vessel' acts as a return electrode for the RFA device providing a current sink within the ablation zone for the RF current to preferentially follow toward lower voltage potential. In the MWA model, the opposite trend is observed whereby tissue temperatures on the vessel side of the thermal array are lower than on the non-vessel side. The authors of this study hypothesize the non-zero thermal conductivity of the stainless steel tube and/or the 'vessel' acting as a passive reflector element within the near field of the ablation probe are responsible for the cooling trend.

In the combined case, thermal behavior along the temperature probe arrays within the RFA and MWA ablation zones is a result of the superposition of thermal and conductive effects. In the RFA case, the conductive effect is initially dominant. The temperatures on the vessel side rise considerably faster than the non-vessel side due to vessel current sink. When the CoolTip™ algorithm begins to pulse energy, noted by the oscillation in temperature, the thermal effect of the vessel begins play a significant role in tissue temperature. By the end of the ablation cycle, the temperature of tissue 5 mm from the electrode has reached symmetry across the thermal array and at 10 mm the non-vessel side is hotter than the vessel side. In the MWA case, the thermal effect of the vessel dominates over the entire ablation cycle, resulting in lower vessel side tissue temperature.

Table II shows whether a statistically significant shift in the ablation boundary radius was observed in the data on both the vessel side and non-vessel side of the thermal array when compared to the control. MWA and RFA energy types had similar statistical results except for the conductive case, where RFA displayed smaller ablation zone radius to the opposite side of the ablation when compared to the control. MWA showed no statistical difference in this case from the control. Table I communicates trends that were consistently observed throughout all measurement trials for the specified energy type/vessel effect. For the thermal case, the MWA and RFA ablation zone radius trended smaller toward the vessel. For the conductive case only RFA showed a trend with the radius on the opposite side of the vessel consistently smaller than the control. In the combined case, RFA ablation zone radius trended smaller on both the vessel side and non-vessel side, whereas MWA only trended small on the vessel side.

V. Conclusion

This study separates the thermal and electrical effects of large vasculature at the edge of an ablation zone for both RFA and MWA energy modalities. The results suggest RFA is susceptible to both the thermal and current sink effects of large vasculature while MWA is only susceptible to thermal sink. Ablation zone boundaries were distorted on both the vessel and non-vessel sides with RFA whereas with MWA only the vessel side is affected.

References

[1] D. Haemmerich, P.F. Laeseke, Thermal tumor ablation: Devices, clinical applications and future directions. *Int. J. Hyperthermia*, December 2005; 21(8): 755-760.

[2] Wood T.H. Lethal effects of high and low temperatures on unicellular organisms. *Advances in Biological Medical Physics* 1956; 4.

[3] Chang I, Nguyen U. Thermal modeling of lesion growth with radiofrequency ablation devices. *BioMed. Eng. OnLine* 2004; 3 (1):27

[4] C.M. Ladtkow, Practical Application of Rate Mediated Ablation Size Estimation, *Conf. Soc. Thermal Med*, April 2007.